A GENUINELY MULTIDISCIPLINARY JOURNAL

CHEMPLUSCHEM

CENTERING ON CHEMISTRY

# Accepted Article

**Title:** Design and Synthesis of Energetic Materials towards Vasatile Applications by N-trinitromethyl, -nitromethyl and -methyl acetate Functionalization of Nitroimidazoles

**Authors:** Xin Yin, Jie Li, Guojie Zhang, Zhenqi Zhang, Qing Ma, Jun Wang, and Shumin Wang



**To be cited as:** *ChemPlusChem* 10.1002/cplu.201800305

**Link to VoR:** http://dx.doi.org/10.1002/cplu.201800305

A Journal of ChemPubSoc Europe

WILEY-VCH

www.chempluschem.org

# Design and Synthesis of Energetic Materials towards Versatile Applications by N-trinitromethyl and N-nitromethyl Functionalization of Nitroimidazoles

Xin Yin, [a][b] Jie Li, [a] Guojie Zhang,[a] Zhenqi Zhang,[a] Qing Ma,* [a] Jun Wang,*[a] and Shumin Wang*[b]

Dedication ((optional))

**Abstract:** The modification of the properties of energetic materials is important not only for getting insight into the relationship between structures and properties but also for multiple applications in reality. In the present investigation, a new family of energetic compounds, polynitroimidazoles featuring trinitromethyl, nitromethyl and methyl acetate moieties at the nitrogen atom of heterocyclic rings were synthesized. The high-energy dense oxidizers 2-nitro and 4-nitro-1-(trinitromethyl)-1H-imidazoles were obtained by nitration of 1-acetonylpolynitroimidazoles in fuming $HNO_3$ and concentrated $H_2SO_4$. 4,5-dinitro-1-(nitromethyl)-1H-imidazole and 4,5-dinitro-1-(acetate methyl)-1H-imidazole were surprisingly afforded by using 68% $HNO_3$ and concentrated $H_2SO_4$ through controllable synthesis. All the intermediates and the target compounds were confirmed by X-ray diffraction. The characterized chemical and physical properties indicate that these new materials show promising energetic performance towards future applications in various industry areas.

## Introduction

The design and synthesis of green energetic materials beyond the current carbon-rich commercial explosives (TATB, TNT) are important goals with decreasing their detonation products of carbon dioxide. There have been numerous attempts to synthesize suitable alternative candidates based on nitrogen-rich frameworks. Among them, imidazole is a significant framework for constructing new drugs, ionic liquids, as well as energetic materials.[1] Polyimidazole derivatives are a series of insensitive energetic materials (2,4-dinitroimidazole, 4,5-dinitroimidazole, 2,4,5-trinitroimidazole, etc.), but their acidity and hygroscopicity behaving in the α-position of heterocycles limits their further strorage and applications.[2] To solve these issues, different N-functionalized polyimidazole derivatives have been prepared by using N-amination, N-methylation and N-nitramination.[3] Meanwhile, ionic salts by metathesis reaction of acidic polyimidazolate anions with nitrogen-rich cations have been prepared.[4]

Earlierly, Semenov et al studied the acetonylation of nitroazoles including nitroimidazole, nitropyrazole, nitrotriazole, nitro-bis-pyrazole as well as nitro-bis-triazole. Afterwards, they synthesized a series of dinitromethyl nitroazole-based compounds. But they did not report the relative energetic properties.[5] Thottempudi et al synthesized of trinitromethyl and dinitromethyl substituted N-methyl-5-nitro-1H-imidazoles and their salts from the starting material (N-methyl-5-nitro-1H-imidazolyl)-acetic acid.[6] Recently, Sheremetev et al reported N-trinitromethyl-substituted polynitropyrazole-based and pyrazole-tetrazole hybrid energetic compounds with evaluation of their possible applications in propellants.[7] To enhance the density and energy of target molecules, Zhang et al further synthesized *gem*-dinitromethylated derivatives of 5,5'-dinitro-bis-1,2,4-triazole and 3-amino-5-nitro-1,2,4-triazole by using the same synthetic strategy.[8] We recently found that 4,5-dicyano-1,2,3-triazole can be successfully substituted with *N*-trinitromethyl group in its α-position but this group could leave once it was used for further cyclization.[9] In the last decades, nitration reactions of carbon-sustituted acetic acid ethyl ester and acetic acid were released as important results and great discoveries.[10] To the best of our knowledge, the influence of different nitration conditions on the target products after the substitution by bromoacetone has not been fully covered.

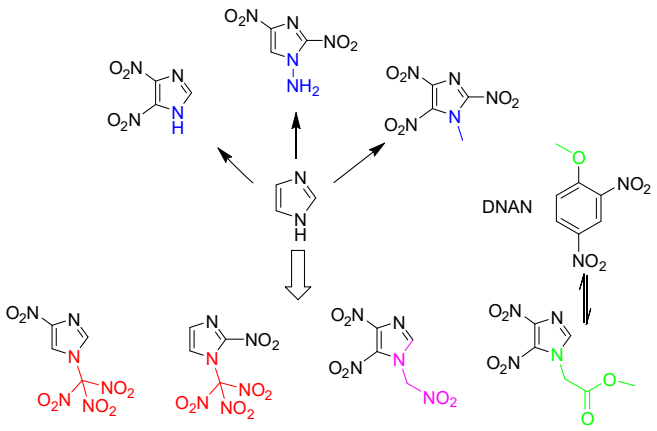


**Scheme 1** Different heterocyclic frameworks containing fluorodinitroethyl moieties *via* substitution in amino groups from imidazole

As shown in Scheme 1, in comparison to methyl, amino substituted polyimidazoles, in this work we introduced other energetic groups or functional groups into polynitroimidazole backbones. Through investigations of methods on nitration of

[a] X. Yin, J. Li, G. Zhang, Dr. Z. Zhang, Dr. Q. Ma*, Prof. J. Wang*
Institute of Chemical Materials
China Academy of Engineering Physics
Mianyang 621900 (P. R. China)
E-mail: maq@caep.cn; wangjun01@caep.cn
[b] X. Yin, Prof. S. Wang*
School of National Defense Science and Technology
Southwest University of Science and Technology
Mianyang 621010 (P. R. China)
E-mail: 727849335@qq.com

Supporting information for this article is given via a link at the end of the document.((Please delete this text if not appropriate))

**Scheme 2.** Synthesis routes for obtaining **3, 4, 5, 6, 9, 10, 13** and **14.**

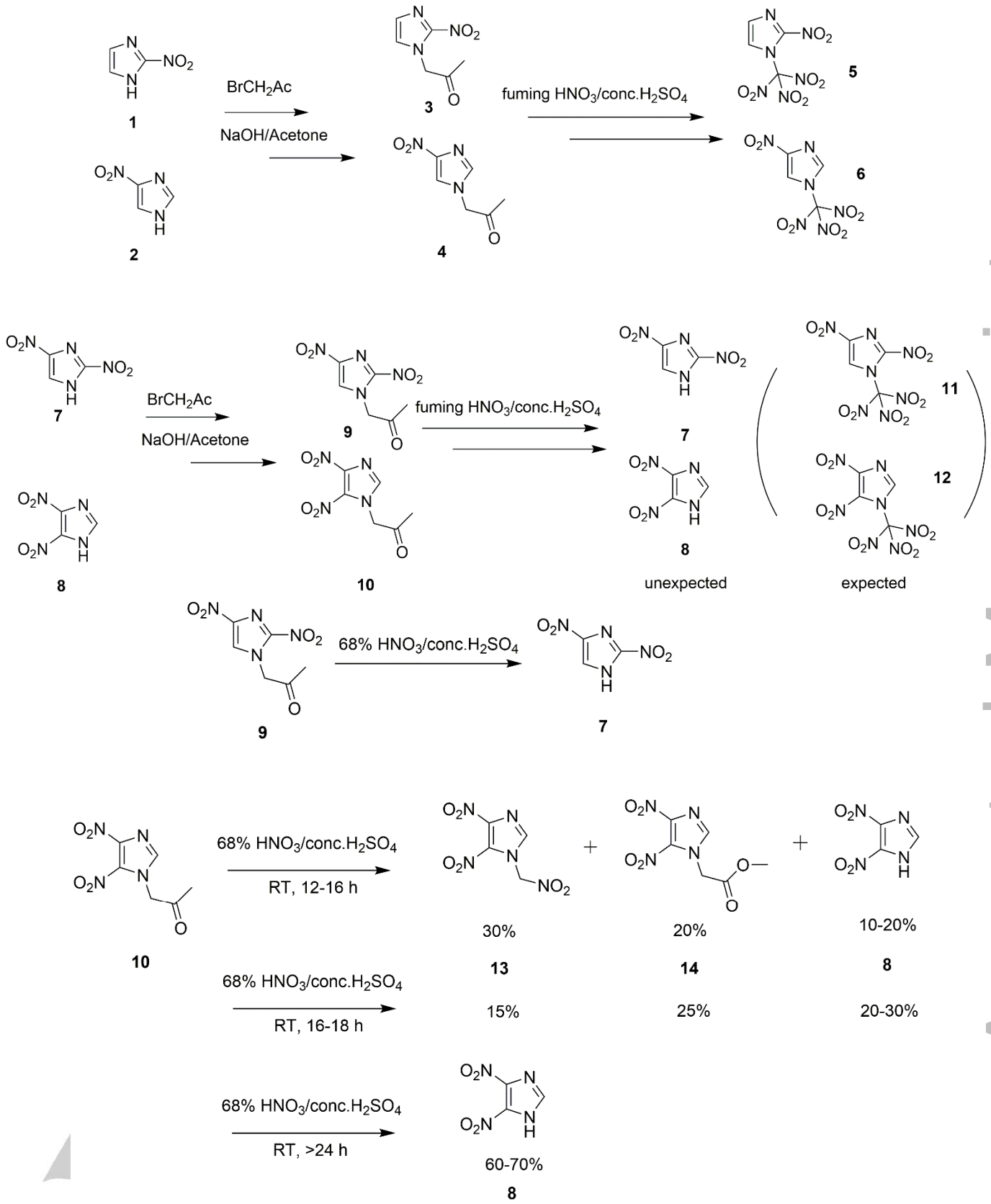

propane-one derivatives, four neutral final compounds were obtained. Interestingly, except for two new oxidizers, another new compound was a melt-cast explosive because of its similar melt-castable structure with commercial 2,4-dinitroanisole (DNAN). Their crystal structures, thermal stability, safety and detonation performance were further characterized. The results indicated that the energetic properties of resultant compounds may be conveniently tuned *via* varying the energetic groups of substituents from trinitromethyl, nitromethyl to acetate methyl.

## Results and Discussion

### Synthesis

As shown in Scheme 2, the synthesis of precusors **3**, **4**, **9** and **10** was performed in the extence of bromoacetone reacting with polyinitroimidazole substrates **1**, **2**, **7**, **8** as the starting materials according to the known methods from literatures.[5] After successfully affording acetonyl imidazoles, they were further used of nitration to achieve the target molecules **5**, **6**, **11** and **12**. As expected, N-trinitromethyl nitroimidazole **5** and its isomer **6** can be obtained by nitration of intermediates **3** and **4** in the mixture of fuming $HNO_3$ and concentrated $H_2SO_4$ in 48 h, giving yield 57% and 61%, respectively. They were both extracted from diluted mixture of acid. Unexpectedly, **11** and **12** could not be affored even with undergoing a prolonged time (2 weeks). Instead, we found that intermediates **9** and **10** all became the starting materials **7** and **8** under different reaction time, respectively. After several attempts by changing the concentration of $HNO_3$ (68%, fuming, 100%) and $H_2SO_4$ (98%, fuming), it was found that under the mixted acid of 68% $HNO_3$ and 98% $H_2SO_4$, intermediate **9** only reacted into its starting material **7**. Fortunately, intermediate **10** could react in this nitration condition. Under the reaction time between 12 h and 16 h, new compound **13** was the major product (yield 30%) together with another new compound **14** (yield 20%) and the starting material **8** (yield 10-20%) by isolation of thin-layer chromatography (TLC). During 16 h and 18 h, new compound **14** was the major product (yield 25%). It should be noted that the overall yield of compound **13** and **14** decreased during this period. After 24 h, only the starting material **8** was obtained (yield 60-70%). These new compounds (**13** and **14**) can be further isolated by column chromatography in different eluants (ethyl acetate: petroleum ether=1:1 for **13;** ethyl acetate: dichloromethane=1:20 **for 14)**.

### Crystal Structures

Tthe single crystals of intermediates **3, 4, 9** and **10** were obtained and determined, which indicated that $BrCH_2Ac$ was successfully substituted into the α-positions in polynitroimidazoles (See the Supporting Information). The target products suitable for single-crystal X-ray diffraction were obtained by slow evaporation of anhydrous methanol or ethanol at ambient temperature. The crystal and structure data of **5, 6, 13** and **14** are listed in Table 1 and Figure 2-5. The other relevant crystal parameters involving selected bond lengths, angles, anisotropic displacement parameters, hydrogen coordinates and isotropic displacement parameters are listed in the Supporting Information.

N-trinitromethyl nitroimidazole **5** crystallizes in the orthorhombic space group *P*bca with sixteen molecules per unit cell and a density of 1.874 g $cm^{-3}$ at 130 K. The molecular structure is depicted in Figure 2a. The bond lengths of C8–N11, C8–N12, C8–N13 are 1.5451(19) Å, 1.5510(19) Å and 1.5435(18) Å respectively, which are longer than normal C–N single bond length, indicating the strong electron-withdrawing effect of nitro groups in trinitromethyl moieties. It is also found that nitro group is basically coplanar with imidazole ring but nitro groups in trinitromethyl are totally twisted from this plane. In the packing diagram of Figure 2b, intermolecular hydrogen bonds cross and lead to a two-dimensional network. The representative intra- and intermolecular hydrogen bonds are illustrated in blue color. Among them, the relatively strong interaction is intermolecular hydrogen bond C–H···O (2.631 Å) between hydrogen atoms in imidazole ring and oxygen atoms in neighouring trinitromethyl groups, intramolecular hydrogen bond C–H···O (2.606 Å) between CH in imidazole and trinitromethyl groups.

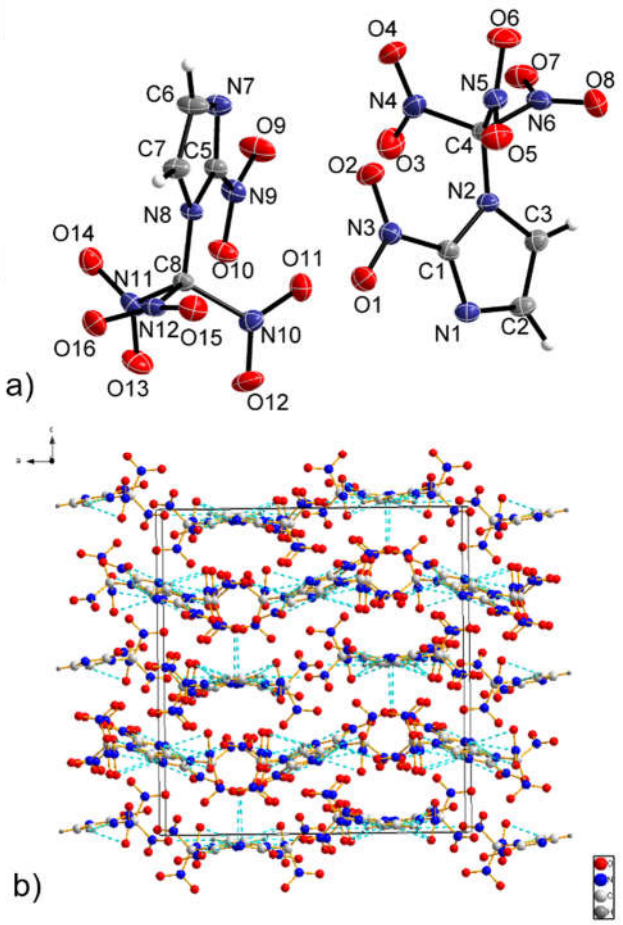

**Table 1.** Crystal data and structure refinement details for **5, 6, 13** and **14.**

| | **5** | **6** | **13** | **14** |
|---|---|---|---|---|
| Formula | $C_4H_2N_6O_8$ | $C_4H_2N_6O_8$ | $C_4H_3N_5O_6$ | $C_6H_6N_4O_6$ |
| Mw [g mol$^{-1}$] | 262.12 | 262.12 | 217.11 | 230.15 |
| T [K] | 130 | 170 | 205 | 173 |
| Crystal size [mm$^3$] | 0.20×0.12×0.05 | 0.25×0.12×0.10 | 0.19×0.15×0.12 | 0.28×0.15×0.12 |
| Crystal system | Orthorhombic | Orthorhombic | Orthorhombic | Monoclinic |
| Space group | *Pbca* | $P2_12_12_1$ | $P2_12_12_1$ | $P2_1/n$ |
| *a* [Å] | 17.7184(16) | 7.0504(16) | 6.3437(11) | 7.2537(12) |
| *b* [Å] | 11.1282(10) | 10.661(3) | 10.1592(18) | 14.416(2) |
| *c* [Å] | 18.8514(17) | 12.070(3) | 24.639(4) | 17.810(3) |
| *α* [º] | 90 | 90 | 90 | 90 |
| *β* [º] | 90 | 90 | 90 | 98.778(5) |
| *γ* [º] | 90 | 90 | 90 | 90 |
| V [Å$^3$] | 3717.0(6) | 907.3(4) | 1587.9(5) | 1840.6(5) |
| Z | 16 | 4 | 8 | 8 |
| λ [Å] | 0.71073 | 0.71073 | 0.71073 | 0.71073 |
| $\rho_{calc}$ [g cm$^{-3}$] | 1.874 | 1.919 | 1.816 | 1.661 |
| *μ* [mm$^{-1}$] | 0.183 | 0.187 | 0.172 | 0.150 |
| *F* (000) | 2112.0 | 528.0 | 880.0 | 944.0 |
| *θ* range [º] | 4.322-61.054 | 5.098-55.336 | 3.306-55.124 | 3.652–52.74 |
| Reflections collected | 35618 / 5673 | 8049 / 2086 | 11931 / 3644 | 12454 / 3728 |
| $R_{int}$ | 0.0578 | 0.0508 | 0.0872 | 0.0692 |
| Data/restraints/parameters | 5673 / 0 / 325 | 2086 / 136 / 164 | 3644 / 12 / 272 | 3728 / 0 / 291 |
| Final R index [I>2σ(I)] | $R_1$=0.0378 | $R_1$=0.0359 | $R_1$=0.0587 | $R_1$=0.0500 |
| | $wR_2$=0.0829 | $wR_2$=0.0721 | $wR_2$=0.1053 | $wR_2$=0.1147 |
| Final R index [all data] | $R_1$=0.0750 | $R_1$=0.0457 | $R_1$=0.1196 | $R_1$=0.0817 |
| | $wR_2$=0.0993 | $wR_2$=0.0769 | $wR_2$=0.1301 | $wR_2$=0.1338 |
| GOF on F$^2$ | 1.002 | 1.008 | 0.980 | 1.026 |
| CCDC number | 1847115 | 1847114 | 1847110 | 1847113 |

**Figure 2.** a) ORTEP representations of single-crystal X-ray structure of **5** shown at the 50% probability level; b) Crystal packing of single-crystal X-ray structure and hydrogen bonds in unit cell for **5** (Dashed lines indicate intra- or intermolecular interacting bonds).

N-trinitromethyl nitroimidazole **6** crystallizes in the orthorhombic space group $P2_12_12_1$ with four molecules per unit cell and a density of 1.919 g cm$^{-3}$ at 170 K. Its crystal structure is shown in Figure 3a. Comparing with its another isomer **5**, it has higher crystal density because the nitro group are not adjacent to the trinitromethyl group due to weak steric stabilization, which thereby produces closer crystal packing. Besides, stronger intramolecular and intermolecular hydrogen bonds are observed in Figure 3b. The intramolecular hydrogen bond lengths of C–H···O are all 2.670 Å between imidazole and nitro group in its 4-position, whereas bond lengths of C–H···O between imidazole and trinitromethyl group are not consistent which range from 2.560 Å to 2.873 Å. The intermolecular hydrogen bond lengths of C–H···O lie in the range of 2.465–2.586 Å, which are basically stronger than those in isomer **5**.

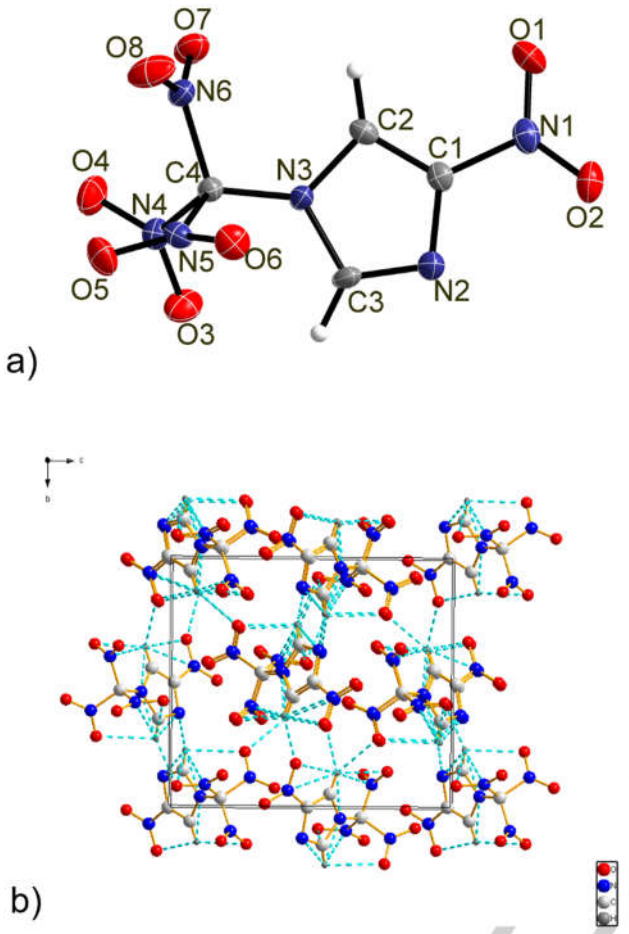


**Figure 3.** a) ORTEP representations of single-crystal X-ray structure of **6** shown at the 50% probability level; b) Crystal packing of single-crystal X-ray structure and hydrogen bonds in unit cell for **6** (Dashed lines indicate intra- or intermolecular interacting bonds).

N-nitromethyl nitroimidazole **13** crystallizes in the orthorhombic space group $P2_12_12_1$ with eight molecules per unit cell and a density of 1.816 g cm$^{-3}$ at 205 K. Its crystal structure is shown in Figure 4a. The C1–N1 bond length (1.436(6) Å) in nitromethyl group is longer than C1–N2 bond length (1.359(6) Å), but slight shorter than C3–N3 (1.440(6) Å) and C4–N5 (1.455(6) Å) bond lengths, suggesting this carbon-nitrogen single bond is stable. While for C1–N1 bond (1.494(6) Å), it is longer than those of other C–N single bond in carbon-nitro groups but still shorter than those of trinitromethyl in **5** and **6** (range of 1.534–1.557 Å). The crystal packing in Figure 4b shows a "wave-like" stacking pattern. **13** still shows a non-coplanar molecule but the incorporation of methylene group increases its hydrogen bonding interaction when comparing with those N-trinitromethyl compounds. In Figure 2b, after being substituted with nitromethyl moiety, intramolecular hydrogen bond C–H···N (1.991 Å) was found. In contrast to N-trinitromethyl group, methylene group also played a significant role as hydrogen bond donor when it is neighboring nitro groups and nitrogen-rich frameworks.

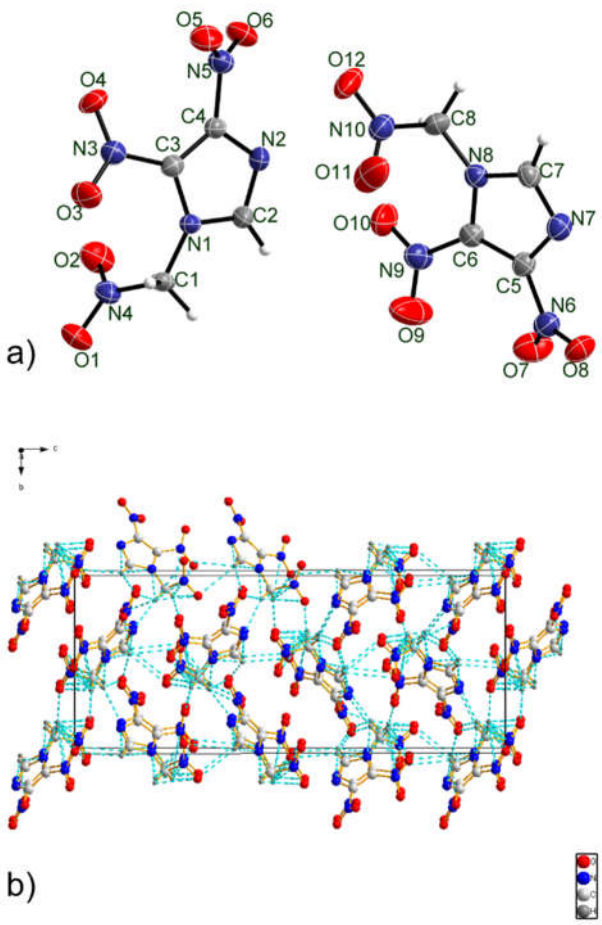


**Figure 4.** a) ORTEP representations of single-crystal X-ray structure of **13** shown at the 50% probability level; b) Crystal packing of single-crystal X-ray structure and hydrogen bonds in unit cell for **13** (Dashed lines indicate intra- or intermolecular interacting bonds).

N-methyl acetate nitroimidazole **14** crystallizes in the monoclinic space group $P2_1/n$ with eight molecules per unit cell and a density of 1.661 g cm$^{-3}$ at 173 K. Its crystal structure is shown in Figure 5a. Due to long chain of methyl acetate group, the whole molecule shows a "chair" like structure. The C4–N3 bond length (1.461(3) Å) is slightly longer than C–N single bond in **13**. In Figure 5b, its crystal packing exhibits a crossing stacking pattern. Because the introduction of methylene and methyl groups, hydrogen bonds increase in contrast to those in **5**, **6** and **13**. After being substituted with methyl acetate moiety, there are two obviously intense intramolecular hydrogen bonds were found, such as C–H···O (2.514 Å) between methylene group and carbonyl group, and C–H···O (2.507 Å) between

methylene group and nitro group in the 5-position of imidazole ring. In comparison with methyl group in its tail-position, methylene group plays more important role as hydrogen bond donor in **14**.

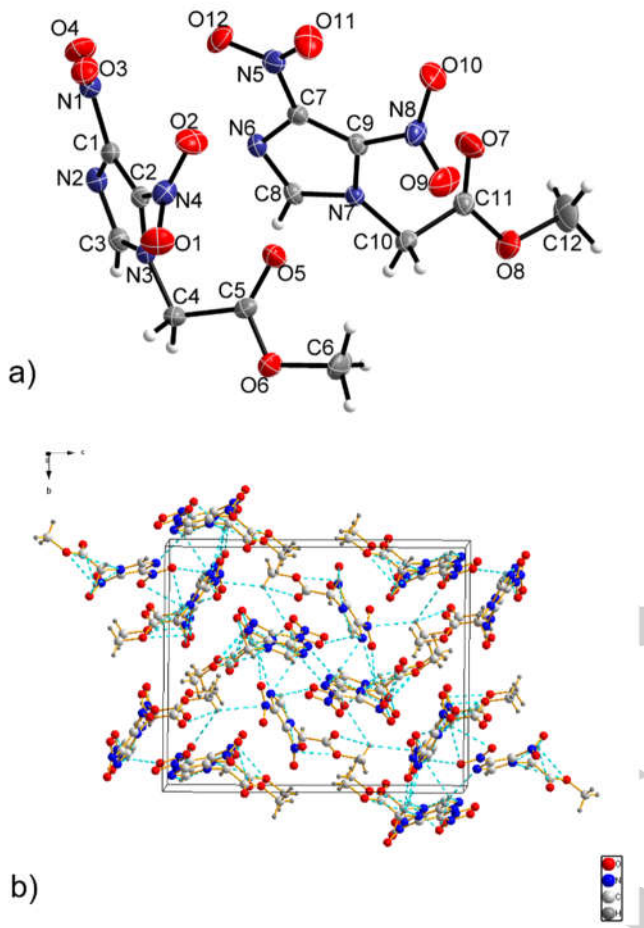


**Figure 5.** a) ORTEP representations of single-crystal X-ray structure of **14** shown at the 50% probability level; b) Crystal packing of single-crystal X-ray structure and hydrogen bonds in unit cell for **14** (Dashed lines indicate intra- or intermolecular interacting bonds).

### Thermal stability and energetic properties

The decomposition temperatures of compounds **5**, **6**, **13** and **14** were measured by using differential scanning calorimetery (DSC) instrument with a heating rate of 5 °C min$^{-1}$ as illustrated in Figure 6. As expected, the decomposition temperature of **5** ($T_d$: 126 °C, $T_p$: 154 °C) and **6** ($T_d$: 119 °C, $T_p$: 145 °C) is lower than 200 °C because N-trinitromethyl group is incorporated. Meanwhile, **5** and **6** show onset melting point from 96 °C and 105 °C, respectively. Without trinitromethyl group, compound **13** shows an improved thermal stability, which starts to melt from 120 °C, decomposes from 147 °C and arrives at the peak of 185 °C. Its thermal properties are similar with nitromethyl substituted pyrazole derivatives recently reported by Shreeve et al.[12e] It is worthy noting that compound **14** exhibits a surprising melting point at 86 °C, onset decomposition temperature from 224 °C, and decomposition peak at 247 °C. This indicates that it is a melt-cast explosive and behaves good thermal stability, which may attribute to its $CH_3O$-C moiety similar with that of DNAN.

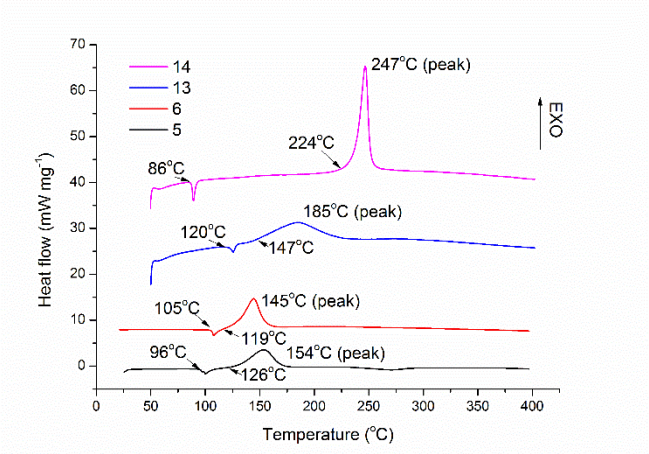


**Figure 6.** DSC curves of **5**, **6**, **13** and **14** measured at the heating rate of 5°C min$^{-1}$.

The oxygen balance (OB) of **5** and **6** (+18.3%) is better than nitroglycerine (NG) (+5.5%) and approaches that of ammonium dinitroamide (ADN) (+26%). Compound **13** exhibits a slightly higher OB than that of RDX, and **14** shows competitively superior OB to that of TNT. Their heat of formation (HOF) were further calculated using the Gaussian 09 (Revision D.01) suite of program,[11] and the energetic properties are summarized in Table 2. Except for **14** (-293.2 kJ mol$^{-1}$), other compounds show positive HOF (58.9-149.8 kJ mol$^{-1}$). Using the values of HOF and their crystal densities at 298 K, detonation parameters were estimated by using EXPLO5 (version 6.02). Compound **5** and **6** has good detonation velocity (*D*) (**5**: 8827 m s$^{-1}$; **6**: 9003 m s$^{-1}$) and detonation pressure (*P*) (**5**: 34.1 GPa; **6**: 36.2 GPa), which are not only significantly superior to those of ADN and NG but also surpass RDX. Though compound **13** shows relatively lower detonation performance than those of RDX, it still can be a good candidate (*D*: 8344 m s$^{-1}$, *P*: 30.1 GPa) for the replacement of NG. In comparison to those of TNT, compound **14** exhibts competitively higher detonation velocity (*D*: 7134 m s$^{-1}$) but slightly lower detonation pressure (*P*: 18.9 GPa), which are all superior to those of DNAN (*D*: ~5600 m s$^{-1}$). As potential propellants, **5**, **6** and **13** show higher specific impulses ($I_{sp}$: 255-266s) than those of ADN (202 s). $I_{sp}$ of **5** and **6** is superior to that of RDX and NG, but **13** shows a slightly lower value than them.

Impact (*IS*) and friction sensitivity (*FS*) values were measured by using an internationally used BAM drophammer instrument and BAM friction tester. **5** and **6** all show poor impact and friction sensitivities (4-4.5 J, 42-48 N) which are comparable to those of ADN and better than NG, but worse than those of RDX. Compound **13** exhibits better *IS* and *FS* values (*IS*: 18 J, *FS*: 120 N) than those of RDX. With respect to those of TNT, compound **14** shows better *IS* and *FS* values (*IS*>40 J, *FS*>360

N), which indicates its potential application in metl-cast formulations.

### Hirshfeld surface analysis and intermolecular interaction

To investigate intermolecular interaction in the molecular crystals, Hirshfeld surface analysis was employed.[13] In the previous study, Shreeve et al have pointed out the correlation between intermolecular interaction and sensitivities of energetic ionic salts existed because of relatively strong intermolecular hydrogen bonds induced by hydrogen-rich cations.[14] On the other hand, Zhang et al studied the differences of commercially used explosives such as TNT, TATB, LLM-105, RDX, HMX and CL-20, which mapped the significant principle of hydrogen bonding interaction existing in the insensitive highly explosives and also found that O•••O became the first occupation in those sensitive explosives.[15] For the new neutral compounds synthesized in this work, to understand the change of different sensitivities measured in Table 2, it is also necessary to investigate their interaction in the real crystals. As shown in Figure 7, three types of contact interaction are given as O•••O, H•••O and O•••H due to the absence of primary or secondary amino group. It is worthy noting that red color region only emerges in the center of fingerprint plot of sensitive compounds **5** and **6**. In addition, Figure 8 further illustrates the concrete distributions of their individual intermolecular interaction. In compound **5** and **6**, O•••O contact interaction dominates the main intermolecular interaction (**5**: 41.9 %, **6**: 47.0%), while H•••O and O•••H interaction contribute 21-33%. For compound **13** and **14**, distributions of H•••O and O•••H interaction (37-57%) surpass those of O•••O contact interaction (**13**: 28.9%, **14**: 9.7%). Relatively high O•••O contact interaction usually represents that oxygen atoms in nitro groups could expose on the molecular surfaces and increases the possibility of unexpected explosion towards mechanical stimuli. While hydrogen bonding interaction becomes the dominating interaction this possibility could decrease. The analysis results by the Hirshfeld surface are basically consistent with experimental results in the safety test, as well as the previously theoretical views proposed by Zhang et al and Shreeve et al.

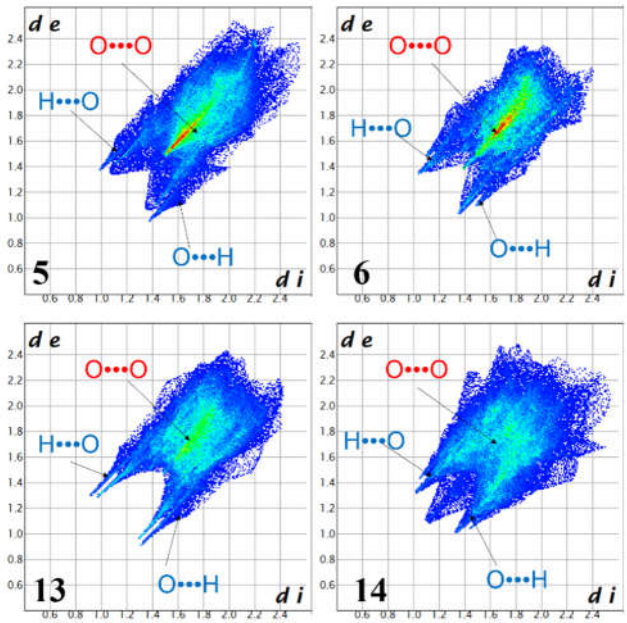


**Figure 7.** Fingerprint plots of **5**, **6**, **13** and **14** as well as main types of intermolecular interaction in their individual molecular crystals.

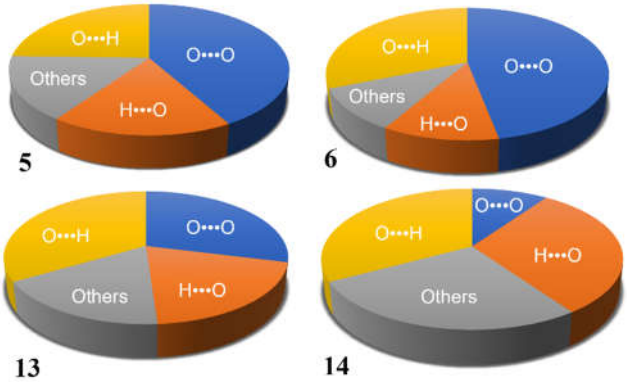

**Figure 8.** Intermolecuar interaction distributions of **5**, **6**, **13** and **14**.

**Table 2** Physical and energetic properties of **5**, **6**, **13** and **14**.

| | **5** | **6** | **13** | **14** | **ADN**[12] | **NG**[12] | **TNT**[12] | **RDX**[12] |
|---|---|---|---|---|---|---|---|---|
| $\rho$ (g cm$^{-3}$)[a] | 1.83 | 1.88 | 1.77 | 1.63 | 1.81 | 1.59 | 1.65 | 1.80 |
| OB (%)[b] | +18.3 | +18.3 | +3.7 | -20.9 | +26 | +5.5 | –74 | 0 |
| $D$ (m s$^{-1}$)[c] | 8827 | 9003 | 8344 | 7134 | 7860 | 7630 | 6881 | 8795 |
| $P$ (GPa)[d] | 34.1 | 36.2 | 30.1 | 18.9 | 23.6 | 22 | 19.5 | 34.9 |
| $\Delta H_f$ (kJ mol$^{-1}$)[e] | 149.8 | 126.1 | 58.9 | -293.2 | -149.8 | -351.5 | –67.0 | 92.6 |
| $T_m$ (°C)[f] | 97 | 105 | 120 | 86 | 93 | 13 | 81 | 204 |
| $T_{dec}$ (°C)[g] | 126 | 119 | 147 | 224 | 159 | 50 | 295 | 210 |
| $IS$ (J)[h] | 4 | 4.5 | 18 | >40 | 3-5 | 0.3 | 15 | 7.4 |
| $FS$ (N)[i] | 42 | 48 | 120 | >360 | 64-72 | – | 240 | 120 |
| $I_{sp}$[j] | 266 | 265 | 255 | 195 | 202 | 259 | 209 | 258 |

[a] Density measured at 298 K; [b] Oxygen balance for $C_aH_bO_cN_d$, 1600(c-a-b/2)/$M_w$, $M_w$=molecular weight; [c] Calculated detonation velocity (EXPLO5 V6.02); [d] Calculated detonation pressure (EXPLO5 V6.02); [e] Calculated heat of formation; [f] Onset melting point measured by DSC/DTA ($\beta$=5°C min$^{-1}$); [g] Onset decomposition temperature measured by DSC/DTA ($\beta$=5°C min$^{-1}$); [h] Impact sensitivity measured by BAM drop-hammer test; [i] Friction sensitivity measured by a BAM friction tester; [j] Specific impulse (EXPLO 5 V6.02).

## Conclusions

Through controllable nitration methods, a series of new N-functionalized polynitroimidazoles were synthesized and their physicochemical properties were modified based on different substituents. The structures of these compounds were determined by single crystal X-ray diffraction. For different purpose, N-trinitromethyl nitroimidazole **5** and its isomer **6** possess high densities (1.83-1.88 g cm$^{-3}$), high positive oxygen balance (+18.3%), high detonation performance (~9000 m s$^{-1}$), high specific impulses (265-266 s) and acceptable sensitivities (*IS*: 4-4.5J, *FS*: 42-48 N), which indicate their potential applications in high energy density oxidizers (HEDOs). N-nitromethyl nitroimidazole **13** show its high detonation performance, low sensitivity (*IS*: 18J, *FS*: 120N) and enhanced thermal stability, which explains that it may be a pratical replacement for NG but an improved syntheitc method is required. For N-methyl acetate nitroimidazole **14**, it exhibits low sensitivities (*IS*>40J, *FS*>360N), good detonation performance (*D*: 7134 m s$^{-1}$) comparing with those of TNT, melt-castable thermal properties (m.p.: 86 °C) with high thermal stability (dec.: 224 °C), which reveals that it can be a good candidate for the replacement of DNAN or even TNT once its synthesis method will be improved in the future work.

## Experimental Section

### Safety Cautions

Although none of the above-mentioned nitrogen-rich energetic materials have exploded or detonated in the procedure of this research, small scale and safety training are strongly encouraged. Mechanical actions such as scratching and scraping must be avoided. Manipulations should be performed behind a safety guard made of polymethyl methacrylate (PMMA). Face shield, mask, eye protection and leather gloves must be worn.

### General methods

All reagents were purchased from TCI or Aladdin in analytical grade and were used as received. $^1$H and $^{13}$C NMR spectra were recorded on a 600 MHz (Bruker AVANCE 600) or 400 MHz (Bruker AVANCE 400) nuclear magnetic resonance spectrometer. Chemical shifts in the $^1$H and $^{13}$C spectra are reported relative to $Me_4Si$. The melting point and decomposition temperature were recorded on a differential scanning calorimeter-thermal gravity (TGA/DSC2, METTLER TOLEDO, STAR$^e$ system) at a heating rate of 5 °C min$^{-1}$. Infrared (IR) spectra were measured on SHIMADZU IRTracer-100 FT-IR spectrometer in the range of 4000–400 cm$^{-1}$ as KBr pellets at 20°C. Elemental analyses (C,H,N) were carried out on a elemental analyzer (Vario EL Cube, Germany) (Though compound **6** was pure, its nitrogen content was outside of the +/- 0.4 % range because the CHN analyses of high nitrogen compounds can be difficult sometimes due to the selection of standard sample). Impact and friction sensitivity measurements were made using a standard BAM Fallhammer and a BAM friction tester, respectively.

**Computational methodology**

The geometric optimization and frequency analysis of compound **5, 6, 13** and **14** were accomplished at the B3LYP/6-311+G(d,p) level.[16,17] The gaseous heat of formation was computed based on the atomization energies were obtained by employing the CBS-4M atomization method or experimental values of small species directly adopted from the NIST Chemistry Webbook[18] and gaseous phase heat of formation was computed *via* isodesmic reactions as shown in Scheme 3.

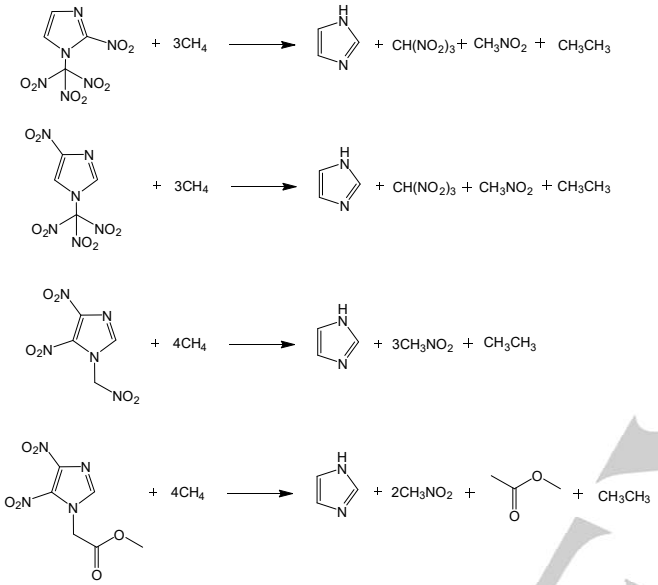


**Scheme 3** Isodesmic reactions for the target compounds

The solid-state heat of formation can be estimated by subtracting the heats of formation from gas-phase heats of formation. For all the reported neutral energetic compounds, the heat of sublimation can be estimated following the Trouton's rule,[19] which is shown in the equation (1):

$$\Delta H_{sub}=188/\text{J mol}^{-1}\text{K}^{-1}T \quad (1)$$

Here, $T$ represents either the melting point or the decomposition temperature when no melting occurs prior to decomposition. Detonation parameters were carried out in the EXPLO5 (V6.02) program[20] using X-ray densities which were converted to room temperature values *via* the following equation:[21]

$$\rho_{298K}=\rho_T/[1+\alpha_v(298-T_0) \quad (3)$$

where the coefficient of volume expansion $\alpha_v$ is $1.5\times10^{-4}$ $K^{-1}$, $\rho_T$ and $T_0$ are the crystal density and the relative temperature, respectively.

**X-ray crystallography**

Suitable crystals of **3**-**6**, **9**, **10**, **13** and **14** were obtained by slow evaporation of their saturated solutions in anhydrous methanol or ethanol. Data were collected on a Bruker three-circle platform diffractometer equipped with a SMART APEX II CCD detector. A kryo-Flex low-temperature device was used to keep the crystals at 130-296 K during data collection. Data collection was performed and the unit cell was initially refined using *APEX2*. Data reduction was carried out using *SAINT* and *XPREP*. Corrections were applied for Lorentz, polarization, and absorption effects using *SADABS*. The structures were further solved and refined with the aid of the programs using direct methods and least-squares minimization by *SHELXS-97* and *SHELXL-97* code.[22] The full-matrix least-squares refinement on $F^2$ involved atomic coordinates and anisotropic thermal parameters for all non-H atoms. The H atoms were included using a riding model. The non-H atoms were refined anisotropically. The finalized CIF files were checked with checkCIF, and deposited at the Cambridge Crystallographic Data Centre (The crystalline parameters were listed in the Supporting Information). Intra- or intermolecular hydrogen-bonding interactions were analyzed with Diamond software (version 3.2 K) as well as the illustrations of molecular structures.

**Syntheses**

**2-nitro-imidazole-1H (1), 4-nitro-imidazole-1H (2), 2,4-dinitroimidazole-1H (7), 4,5-dinitroimidazole-1H (8)** were synthesized according to the literature.[2]

**General procedure for 1-(polyimidazole)-propan-2-one derivatives (3, 4, 9, 10):**[5a]

A solution of bromoacetone (1.1 eq) in acetone (15 mL for 15 mmol) was added to a solution of polynitro-imidazoles (1 eq) and NaOH (1.1 eq) in water (25 mL for 15 mmol). The resulting solution was stirred for another 24 h at ambient temperature. Then a precipitate was filtered and washed with water (5 mL), dried under vacuum to give the relative intermediates (yield 70-85%).

**2-nitro-1-(trinitromethyl)-1H-imidazole** (**5**). To a mixture of fuming $HNO_3$ (15 mL) and concentrated $H_2SO_4$ (20 mL), compound (**3**) (1.8 g, 11 mmol) was added with portions below 0 °C and stirred for 1 h at this temperature. Then the mixture was stirred for 48 h at the room temperature and poured into ice water (100 mL). The white precipitate was filtered, washed with water and dried in vacuum to give an amorphous solid, and **5** was recrystallized in ethanol (1.58 g, yield 57 %). $T_m$: 96°C, $T_d$: 105°C. $^1$H NMR (DMSO-$d_6$, 600.17 MHz): $\delta$=8.65 (s, 1H), 7.94 (s, 1H) ppm; $^{13}$C NMR(DMSO-$d_6$, 150.91 MHz): $\delta$=132.07, 130.10, 129.35, 128.75 ppm; IR (KBr pellet): 3429, 3152, 3124, 2922, 2338, 1633, 1616, 1600, 1566, 1538, 1465, 1384, 1357, 1306, 1286, 1048, 820, 798, 774, 692, 632 cm$^{-1}$. Elemental analysis for $C_4H_2N_6O_8$ (261.99): C 18.33, H 0.77, N 32.07; found: C 18.65, H 0.46, N 33.35.

**4-nitro-1-(trinitromethyl)-1H-imidazole** (**6**). To a mixture of fuming $HNO_3$ (15 mL) and concentrated $H_2SO_4$ (20 mL), compound (**4**) (1.8 g, 11 mmol) was added with portions below 0

°C and stirred for 1 h at this temperature. Then the mixture was stirred for 48 h at the room temperature and poured into ice water (100 mL). The clear solution was extracted with dichloromethane (50 mL×3) and the organic phase was washed with water (20 mL×3). Then the organic phase was dried over magnesium sulfate and the solvent was evaporated. **6** was recrystallized in ethanol (1.72 g, yield 61 %). $T_m$: 105°C, $T_d$: 119°C. $^1$H NMR (DMSO-$d_6$, 600.17 MHz): $\delta$=9.35 (s, 1H), 8.77 (s, 1H) ppm; $^{13}$C NMR(DMSO-$d_6$, 150.91 MHz): $\delta$=148.75, 139.59, 123.34 ppm; IR (KBr pellet): 3434, 3164, 3128, 2923, 1624, 1607, 1565, 1525, 1500, 1400, 1366, 1290, 1265, 1177, 1038, 927, 836, 820, 797, 739, 648 cm$^{-1}$. Elemental analysis for $C_4H_2N_6O_8$ (261.99): C 18.33, H 0.77, N 32.07; found: C 18.70, H 0.14, N 36.55.

**4,5-dinitro-1-(nitromethyl)-1H-imidazole** (**13**). To 68% $HNO_3$ (6 mL) and concentrated $H_2SO_4$ (4 mL) was added compound (**10**) (1.07 g, 5 mmol) with portions below 0°C. After addition, the mixture was stirred for another 1h at 0–5 °C. Subsequently, the mixture was stirred for another 12-16 h at the room temperature. Then the clear solution was poured into ice water (50 g) under stirring and the precipitate was filtered under vacuum. Compound **13** (0.33 g, 30%) was isolated as a yellow solid by column chromatography (ethyl acetate/petroleum ether=1/1). $T_m$: 120°C, $T_d$: 147°C. $^1$H NMR (DMSO-$d_6$, 400.13 MHz): $\delta$=8.43 (s, 1H), 6.93 (s, 2H) ppm; $^{13}$C NMR(DMSO-$d_6$, 100.61 MHz): $\delta$=139.78, 137.76, 124.68, 78.36 ppm; IR (KBr pellet): 3423, 3134, 3059, 2964, 1589, 1571, 1537, 1492, 1379, 1344, 1292, 1207, 850, 802, 738, 698, 607 cm$^{-1}$. Elemental analysis for $C_4H_3N_5O_6$ (217.00): C 22.13, H 1.39, N 32.26; found: C 22.09, H 1.13, N 29.99.

**4,5-dinitro-1-(acetate methyl)-1H-imidazole** (**14**). To 68% $HNO_3$ (6 mL) and concentrated $H_2SO_4$ (4 mL) was added compound (**10**) (1.07 g, 5 mmol) with portions below 0°C. After addition, the mixture was stirred for another 1h at 0–5 °C. Subsequently, the mixture was stirred for another 16-18 h at the room temperature. Then the clear solution was poured into ice water (50 g) under stirring and the precipitate was filtered under vacuum. Compound **14** (0.29 g, 25%) was isolated as a pale yellow solid by column chromatography (ethyl acetate/dichloromethane=1/20). $T_m$: 86°C, $T_d$: 224°C. $^1$H NMR (DMSO-$d_6$, 400.13 MHz): $\delta$=8.22 (s, 1H), 5.37 (s, 2H), 3.76 (s, 3H) ppm; $^{13}$C NMR(DMSO-$d_6$, 100.61 MHz): $\delta$=167.53, 138.34, 53.48, 49.63 ppm; IR (KBr pellet): 3423, 3116, 1741, 1541, 1490, 1381, 1342, 1296, 1249, 1228, 981, 848, 819, 729, 704, 661 cm$^{-1}$. Elemental analysis for $C_6H_6N_4O_6$ (230.13): C 31.31, H 2.63, N 24.35; found: C 32.43, H 2.76, N 23.01.

## Supporting Information

The supporting information contains detailed crystallographic data of **3**–**6**, **9**, **10**, **13** and **14**.

## *Acknowledgements*

We thank the NSAF Foundation of National Natural Science Foundation of China and China Academy of Engineering Physics (Grant No. U1530262), the Science Challenge Project (TZ2018004), the National Natural Science Foundation of China (Grant No. 11402237) and the Science and Technology Development Foundation of China Academy of Engineering Physics (Grant No. 2015B0302055) for financial support.

**Keywords:** energetic materials • polynitroimidazole • oxidizer • melt-cast explosive • modification

[1] a) A. Koul, E. Arnoult, N. Lounis, J. Guillemont, K. Andries, *Nature* **2011**, *469*, 483–490; b) Q. Zhang, J. M. Shreeve, *Chem. Rev.* **2014**, *114*, 10527–10574; c) J. P. Agrawal, *High Energy Materials: Propellants, Explosives and Pyrotechnics,* Wiley-VCH, 1st ed., Weinheim, **2008**; d) T. M. Klapötke, *Chemistry of High-Energy Materials,* De Gruyter, 3rd ed., Berlin, **2015**.

[2] a) R. Duddu, P. R. Dave, R. Damavarapu, R. Surapaneni, D. Parrish, *Synth. Commun.* **2009**, *39*, 4282–4288; b) J. R. Cho, K. J. Kim, S. G. Cho, J. K. Kim, *J. Heterocyc. Chem.* **2001**, *38*, 141–147; c) S. G. Cho, J. R. Cho, E. M. Goh, J. K. Kim, *Propellants, Explos. Pyrotech.* **2005**, *30*, 445–449; d) J. Wang, H. Dong, X. Zhang, J. Zhou, X. Zhang, J. Li, *Chin. J. Energ. Mater.* **2010**, *18*, 728–729; e) R. Lewczuk, *Propellants, Explos. Pyrotech.* **2018**, *43*, 436–444.

[3] a) R. Duddu, P. R. Dave, R. Damavarapu, N. Gelber, D. Parrish, *Tetrahedron Lett.* **2010**, *51*, 399–401; b) P. Yin, Q. Zhang, J. Zhang, D. A. Parrish, J. M. Shreeve, *J. Mater. Chem. A* **2013**, *1*, 7500–7510; c) P. Yin, J. M. Shreeve, *Angew. Chem. Int. Ed.* **2015**, *54*, 14513–14517; *Angew. Chem.* **2015**, *127*, 14721–14725; d) P. Yin, C. He, J. M. Shreeve, *Chem. Eur. J.* **2016**, *22*, 2108–2113; e) D. Chand, C. He, L. A. Mitchell, D. A. Parrish, J. M. Shreeve, *Dalton Trans.* **2016**, *45*, 13827–13833; f) C. He, P. Yin, L. A. Mitchell, D. A. Parrish, J. M. Shreeve, *Chem. Commun.* **2016**, *52*, 8123–8126; g) Q. Ma, H. Lu, L. Liao, G. Fan, J. Huang, *J. Energ. Mater.* **2017**, *35*, 239–249.

[4] a) H. Gao, C. Ye, O. M. Gupta, J. Xiao, M. A. Hiskey, B. Twamley, J. M. Shreeve, *Chem. Eur. J.* **2007**, *13*, 3853–3860; b) T. M. Klapötke, A. Preimesser, J. Stierstorfer, *Z. Anorg. Allg. Chem.* **2012**, *638*, 1278–1286 ; c) M. M. Breiner, D. E. Chavez, D. A. Parrish, *Synlett* **2013**, *24*, 519–521 ; d) T. M. Klapötke, P. C. Schmid, S. Schnell, J. Stierstorfer, *J. Mater. Chem. A* **2015**, *3*, 2658–2668; e) T. M. Klapötke, P. C. Schmid, S. Schnell, J. Stierstorfer, *Chem. Eur. J.* **2015**, *21*, 9219–9228; f) Q. Ma, Y. Chen, L. Liao, H. Lu, G. Fan, J. Huang, *Dalton Trans.* **2017**, *46*, 7467–7479; g) Q. Ma, G. Fan, L. Liao, H. Lu, Y. Chen, J. Huang, *ChemPlusChem* **2017**, *82*, 474–482.

[5] a) V. V. Semenov, B. I. Ugrak, S. A. Shevelev, M. I. Kanishchev, A. T. Baryshnikov, A. A. Fainzil'berg, *Izv. Akad. Nauk, Ser. Khim.* **1990**, *8*, 1827–1837 ; b) V. V. Semenov, S. A. Shevelev, A. B. Bruskin, M. I. Kanishchev, A. T. Baryshnikov, *Russ. Chem. Bull.* **2009**, *10*, 2014–2033 ; c) V. V. Semenov, S. A. Shevelev, *Mendeleev, Commun.* **2010**, *20*, 332–334.

[6] V. Thottempudi, T. K. Kim, K.-H. Chung, J. S. Kim, *Bull. Korean Chem. Soc.* **2009**, *30*, 2152–2154.

[7] a) I. L. Dalinger, I. A. Vatsadze, T. K. Shkineva, A. V. Kormanov, M. I. Struchova, K. Yu. Suponitsky, A. A. Bragin, K. A. Monogarov, V. P. Sinditskii, A. B. Sheremetev, *Chem. Asian J.* **2015**, *10*, 1987–1996; b) I. L. Dalinger, A. V. Kormanov, K. Yu. Suponitsky, N. V. Muravyev, A. B. Sheremetev, *Chem. Asian J.* **2018**, *13*, 1165–1172.

[8] a) S. Huang, J. Tian, X. Qi, K. Wang, Q. Zhang, *Chem. Eur. J.* **2017**, *23*, 12787–12794; b) T. Liu, X. Qi, K. Wang, J. Zhang, W. Zhang, Q. Zhang, *New J. Chem.* **2017**, *41*, 9070–9076.

[9] X. Yin, J. Li, G. Zhang, H. Gu, Q. Ma, S. Wang, J. Wang, *J. Therm. Anal. Calorim.* **2018**, https://doi.org/10.1007/s10973-018-7390-9.

[10] a) V. Thottempudi, H. Gao, J. M. Shreeve, *J. Am. Chem. Soc.* **2011**, *133*, 6464–6471 ; b) R. Haiges, K. O. Christe, *Inorg. Chem.* **2013**, *52*, 7249–7260 ; c) M. A. Kettner, T. M. Klapötke, *Chem. Commun.* **2014**, *50*, 2268–2270 ; d) M. A. Kettner, K. Karaghiosoff, T. M. Klapötke, M. Sućeska, S. Wunder, *Chem. Eur. J.* **2014**, *20*, 7622–7631; e) Q. Ma, H. Gu, J. Huang, F. Nie, G. Fan, L. Liao, W. Yang, *New J. Chem.* **2018**, *42*, 2376–2380; f) H. Gu, Q. Ma, S. Huang, Z. Zhang, Q. Zhang, G. Cheng, H. Yang, G. Fan, *Chem. Asian J.* **2018**, https://doi.org/10.1002/asia.201800722.

[11] M. J. Frisch, G. W. Trucks, H. B. Schlegel, G. E. Scuseria, M. A. Robb, J. R. Cheeseman, G. Scalmani, V. Barone, B. Mennucci, G. A. Petersson, H. Nakatsuji, M. Caricato, X. Li, H. P. Hratchian, A. F. Izmaylov, J. Bloino, G. Zheng,J. L. Sonnenberg, M. Hada, M. Ehara, K. Toyota, R. Fukuda, J. Hasegawa, M. Ishida, T. Nakajima, Y. Honda, O. Kitao, H. Nakai, T. Vreven, J. A. Montgomery Jr, J. E. Peralta, F. Ogliaro, M. Bearpark, J. J. Heyd, E. Brothers, K. N. Kudin, V. N. Staroverov, T. Keith, R. Kobayashi, J. Normand, K. Raghavachari, A. Rendell, J. C. Burant, S. S. Iyengar, J. Tomasi, M. Cossi, N. Rega, J. M. Millam, M. Klene, J. E. Knox, J. B. Cross, V. Bakken, C. Adamo, J. Jaramillo, R. Gomperts, R. E. Stratmann, O. Yazyev, A. J. Austin, R. Cammi, C. Pomelli, J. W. Ochterski, R. L. Martin, K. Morokuma,V. G. Zakrzewski, G. A. Voth, P. Salvador, J. J. Dannenberg, S. Dapprich, A. D. Daniels, O. Farkas, J. B. Foresman, J. V. Ortiz, J. Cioslowski and D. J. Fox, Gaussian 09 D.01, Gaussian Inc., Wallingford, CT, **2010**.

[12] a) T. M. Klapötke, T. G. Witkowski, *ChemPlusChem* **2016**, *81*, 357–360; b) T. M. Klapötke, M. Leroux, P. C. Schmid, J. Stierstorfer, *Chem. Asian J.* **2016**, *11*, 844–851; c) T. M. Klapötke, M. Q. Kurz, R. Scharf, P. C. Schmid, J. Stierstorfer, M. Sućeska, *ChemPlusChem* **2015**, *80*, 97–106; d) T. T. Vo, D. A. Parrish, J. M. Shreeve, *J. Am. Chem. Soc.* **2014**, *136*, 11934–11937; e) D. Kumar, G. H. Imler, D. A. Parrish, J. M. Shreeve, *J. Mater. Chem. A* **2017**, *5*, 10437–10441; f) Q. Ma, Z. Lu, L. Liao, J. Huang, D. Liu, J. Li, G. Fan, *RSC Adv.* **2017**, *7*, 38844–38852.

[13] a) M. A. Spackman, D. Jayatilaka, *CrystEngComm* **2009**, *11*, 19–32 ; b) M. A. Spackman, J. J. McKinnon, *CrystEngComm* **2002**, *4*, 378–392.

[14] a) J. Zhang, Q. Zhang, T. T. Vo, D. A. Parrish, J. M. Shreeve, *J. Am. Chem. Soc.* **2015**, *137*, 1697–1704; b) J. Zhang, L. A. Mitchell, D. A. Parrish, J. M. Shreeve, *J. Am. Chem. Soc.* **2015**, *137*, 10532–10535; c) J. Zhang, J. M. Shreeve, *J. Phys. Chem. C* **2015**, *119*, 12887–12895; d) P. Yin, L. A. Mitchell, D. A. Parrish, J. M. Shreeve, *Chem. Asian J.* **2017**, *12*, 378–384.

[15] a) Y. Ma, A. Zhang, C. Zhang, D. Jiang, Y. Zhu, C. Zhang, *Cryst. Growth Des.* **2014**, *14*, 4703–4713; b) Y. Ma, A. Zhang, X. Xue, D. Jiang, Y. Zhu, C. Zhang, *Cryst. Growth Des.* **2014**, *14*, 6101–6114; c) L. Meng, Z. Lu, Y. Ma, X. Xue, F. Nie, C. Zhang, *Cryst. Growth Des.* **2016**, *16*, 7231–7239.

[16] J. P. Perdew, K. Burke, M. Ernzerhof, *Phys. Rev. Lett.* **1996**, *77*, 3865.

[17] S. Grimme, *J. Comput. Chem.* **2006**, *27*, 1787.

[18] P. J. Linstrom, W. G. Mallard, Eds. NIST Chemistry WebBook, NIST Standard Reference Database, 69, National Institute of Standards and Technology, **2005**.

[19] a) F. Trouton, *Philos. Mag.* **1884**, *18*, 54–57; b) P. Atkins, Physical Chemistry, Oxford University Press, **1978**.

[20] M. Sućeska, EXPLO5, version 6.02, **2013**.

[21] a) C. Xue, J. Sun, B. Kang, Y. Liu, X. Liu, G. Song and Q. Xue, *Propellants, Explos., Pyrotech.* **2010**, *35*, 333–339; b) D. Fischer, T. M. Klapötke, M. Reymann, J. Stierstorfer and M. B. R. Völkl, *New J. Chem.* **2015**, *39*, 1619–1627.

[22] a) G. M. Sheldrick, SHELXS-97, Program for solution of crystal structures, University of Gottingen, Germany, **1997**; b) G. M. Sheldrick, SHELXL-97, Program for refinement of crystal structures, University of Gottingen, Germany, **1997**.

10.1002/cplu.201800305



WILEY-VCH

**Entry for the Table of Contents** (Please choose one layout)

Layout 1:

## FULL PAPER

A new family of energetic neutral derivatives towards versatile applications based on polynitroimidazole backbones were synthesized and fully characterized. Their physicochemical properties were also investigated.

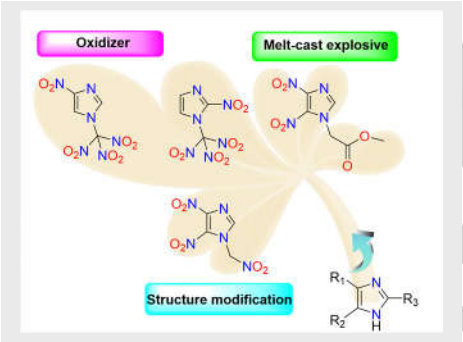


*Xin Yin, Jie Li, Guojie Zhang, Zhenqi Zhang, Qing Ma, Jun Wang, Shumin Wang*

***Page No. – Page No.***
**Design and Synthesis of Energetic Materials towards Versatile Applications by N-trinitromethyl and N-nitromethyl Functionalization of Nitroimidazoles**